GENERATION AND EVOLUTION OF LONGSHORE SANDBARS: MODEL INTERCOMPARISON AND EVALUATION

Tiago Abreu[1], Francisco Sancho[2], Paulo A. Silva[3]

Abstract

Understanding the interaction between waves and currents in coastal waters and to study their influence on the coastal morphology is of great importance for coastal management. In this paper the ability of several practical sediment transport models is assessed to predict beach profile evolutions. For that purpose, the numerical results of a morphodynamic model are compared against the observed beach profile evolutions during the European project "Large Installations Plan" (LIP), using the measured cross-shore velocity data. The results evidence that the classical energetics model of Bailard (1981) provide the best estimates of bed-profile evolution, under erosive wave conditions, when compared to other four sediment transport predictors. However, the use of more recent models (Nielsen, 2006 and Abreu *et al.*, 2013) also shows that a good estimator of the undertow seems to be crucial in such morphodynamic computations..

Key words: morphodynamic modeling, sediment transport, hydrodynamics, undertow, nonlinearities

1. Introduction

Nowadays, one verifies, even to a world scale, coastal management problems associated to littoral morphological changes. The transformations of the coastal zones affect, in medium and long-terms, the stability of the shoreline. However, the processes that intervene in sediment transport are complex (*e.g.*, forces at mobile beds, sediment-flow interactions) and the spatial-temporal scales involved in shoreline and coastal geomorphological evolution are wide (from local to regional scales and spanning from daily, weekly, seasonal, decadal, ... to millennium time-scales). Due to the importance of this issue, and often motivated by undesirable morphologic changes, the scientific community has been engaged in improving their understanding and modeling capabilities of beach morphodynamics. Though several progresses have been made in the past decades, this issue remains a challenge to researchers.

The prediction of morphological changes and sediment budgets in the coastal zone may be obtained from numerical simulation of hydrodynamic and sediment transport processes. It can be verified that as ocean surface waves approach the coast and propagate into shallower water they transform in appearance, becoming asymmetric and skewed (Elgar and Guza, 1985; Doering and Bowen, 1995). While in deep waters the free-surface and wave orbital velocity correspond closely to those of linear waves, *i.e.*, they can be accurately described by a sinusoidal function, in the shoaling zone they become more peaked at the crest and flatter at the trough. Hence, the orbital velocity presents skewness. In the inner surf zone and swash, past wave breaking, a rapid change in the wave orbital velocity during the steep wave front gives rise to large fluid accelerations, while, at the sloping rear face of the wave, the corresponding flow accelerations are much smaller. This asymmetry of the wave leads to acceleration-skewed orbital motions. These transformations from velocity-skewed in the shoaling zone, to acceleration-skewed in the inner surf and swash zone have been measured in laboratory experiments (*e.g.*, Abreu *et al.*, 2011; Sancho *et al.*, 2011) and natural beaches (*e.g.*, Elfrink *et al.*, 2006; Ruessink *et al.*, 2009; Rocha *et al.*, in press). These local nonlinearities are reflected on the near-bed oscillatory flow and are directly linked to sediment transport,

[1]CESAM & Department of Civil Engineering, Polytechnic Institute of Viseu, 3504-510 Viseu, Portugal. tabreu@estv.ipv.pt
[2]Hydraulics and Environment Department, National Laboratory for Civil Engineering, 1700-066 Lisboa, Portugal. fsancho@lnec.pt
[3]CESAM & Department of Physics, University of Aveiro, 3810-193 Aveiro, Portugal. psilva@ua.pt

causing erosion-accretion patterns and bar migration (Hoefel and Elgar, 2003). Another mechanism associated with sediment transport and bar formation is the presence of long infragravity waves (e.g., Holman and Bowen, Baldock et al., 2010). Prel et al. (2011) also recognize that standing wave patterns contribute to the modulation of skewness and asymmetry which lead to morphological evolution, but the mechanisms associated with free long waves are not addressed in this paper.

Different approaches can be undertaken to model the coupled evolution of sea bed topography and the wave current field. The proposed morphodynamic model considers the intra-wave approach, whereby the sediment transport processes are resolved for each individual wave cycle and integrated through time to obtain results at larger time scales, retaining in its formulation as much of the physics of the system as possible (e.g., wave non-linearities and undertow). Whereas the near-bottom seaward directed mean flows (undertow currents) play a crucial role in transporting sediment in the offshore direction, the nonlinearities associated to the wave motion can drive sediment transport in the onshore direction. This work analyses the effects of the wave hydrodynamics interacting with the sea floor in the direction of wave propagation, resulting into a two-dimensional cross-shore analysis (2D). Therefore, it contributes to the cross-shore transport problem, particularly, for the modeling of longshore sandbars in shallow waters.

The accuracy of the results depends largely on the correct simulation of the hydrodynamic and sediment transport processes. Several practical transport formulas are validated against measurements performed in the field and in laboratory facilities. In the present work, the ability of some (practical) sediment transport models (Bailard, 1981; Hoefel and Elgar, 2003; Silva *et al*., 2006; Nielsen, 2006; Abreu *et al*., 2013) is assessed to predict beach profile evolutions. In order to achieve that goal, the numerical results of the morphodynamic model are compared against the observed beach profile evolutions during the European project "Large Installations Plan" (LIP), using the measured cross-shore velocity data (Arcilla *et al*., 1994). The results enable to evidence the relative strength of mechanisms associated with the wave and current-induced sand transports, as well as of the capacities and weaknesses of the present (empirical) practical transport models.

2. LIP Experiments

Within the framework of the European project "Large Installation Plan" (LIP), some experiments were carried out in the 240 m Delta flume of Deltares (formerly Delft Hydraulics) from April to June 1993. The purpose of the study was to generate high quality and high resolution data of hydrodynamics and sediment transport dynamics on a natural beach under equilibrium, erosive and accretive conditions (Arcilla *et al*., 1994; Roelvink and Reniers, 1995). During the experiments, morphological changes were measured along with several physical parameters, such as wave heights, flow velocities and suspended sediment concentrations. In this study, the LIP 1B case is investigated, corresponding to an erosive case where a breaker bar in the surf zone migrates offshore.

At the wave maker location (x=200 m), with a still water depth of 4.1 m, irregular waves were generated according to a Jonswap spectrum with a significant wave height of 1.4 m and a peak period of 5 s. The bed material was uniform sand along the beach profile with a median grain size of d_{50}= 0.22 mm.

The measured values of the significant wave height, H_s, the depth-averaged undertow, U_b, and the bed elevation, z_b, at the beginning of the experiments along the flume are presented in Figure 1. From right to left, in the upper panel, one observes a constant decay of H_s corresponding to a dissipative beach where the incident waves are dissipated within the surf zone. Concerning the undertow, as expected, negative values are always present since this is an offshore directed current which is the result of a mass-flux compensation that balances the mass transported onshore by strongly nonlinear and breaking waves within the shoaling and surf zones. Its magnitude is particularly relevant in the inner surf zone, specially, at the crest of the sand bar ($x = 40$ m) where larger values are attained. The dashed lines plotted over the measured values correspond to linear interpolated values that are used as input at each grid point in the morphodynamic computations.

Figure 2 shows the measured morphological evolution of the sand bar during the simulating period of 18 hr. A seaward migration of its crest of about 10 m was observed. The convergence of the sediment transport, leading to the migration of the bar, results from a balance between the combined effects of non-linear waves, promoting onshore sediment transport, and undertow currents, leading to offshore transport.
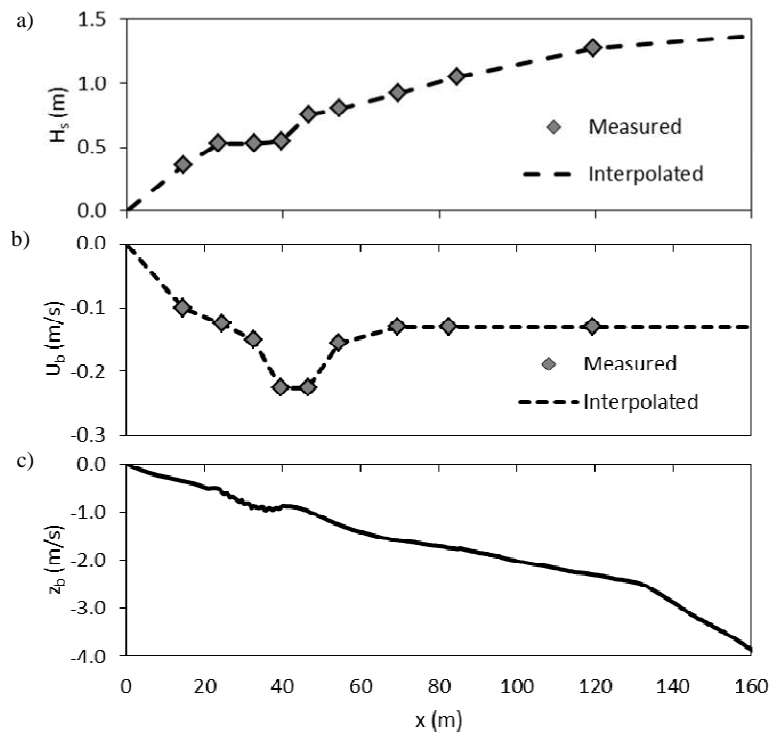
Figure 1. (a) Significant wave height H_s, (b) undertow and (c) bed elevation z_b *versus* cross-shore distance *x*. Diamonds indicate measured values whereas the dotted lines correspond to linear interpolations between these values.
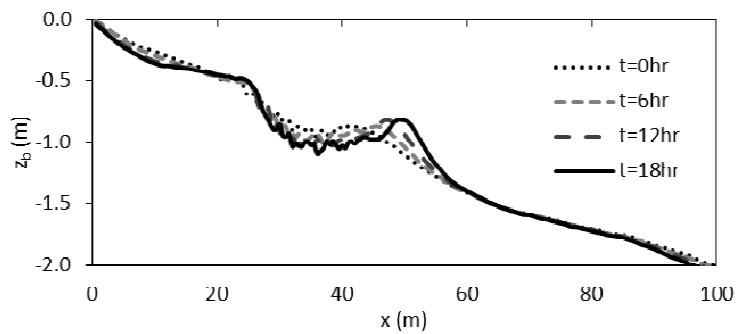

Figure 2. Measured bed elevation z_b *versus* cross-shore distance *x* for 18 hours of simulation. $z_b = 0$ corresponds to mean sea level.

3. Cross-shore morphodynamics

3.1. *Hydrodynamics*

To characterize the horizontal orbital velocity, *u(t)*, under waves with skewness and asymmetry, the present paper uses the analytical description presented by Abreu *et al.* (2010). The formula contains four free parameters: two related to the near-bed orbital velocity amplitude, U_w, and wave angular frequency, ω, and two related to the velocity and acceleration skewnesses, namely, an index of skewness, *r*, and a waveform parameter, ϕ:

$$u(t) = U_w f \frac{\sin(\omega t) + \dfrac{r\sin\phi}{1+f}}{1 - r\cos(\omega t + \phi)} . \tag{1}$$

Here, f is a dimensionless factor , $f = \sqrt{1 - r^2}$.

It is possible to find several publications in the literature enabling the practical application of this formulation, relating the parameters r and ϕ with standard outputs of nearshore hydrodynamic models as the significant wave height, H_s, wave period, T, and water depth, h (*e.g.*, Dibajnia *et al.*, 2001; Elfrink *et al.*, 2006; Ruessink *et al.* 2012). In this work, local values for the nonlinear parameters are computed according to Ruessink *et al.* (2012). These authors provide expressions to obtain r and ϕ as function of the Ursell number, U_r, and a dimensionless non-linearity parameter B:

$$U_r = \frac{3}{8} \frac{Hk}{(kh)^3} , \tag{2}$$

$$B = p_1 + \frac{p_2 - p_1}{1 + \exp\left(\frac{p_3 - \log U_r}{p_4}\right)} . \tag{3}$$

where k is the wave number and $p_1 = 0$, $p_2 = 0.857$, $p_3 = -0.471$ and $p_4 = 0.297$.

Figure 3 shows the spatial variation of U_w, r, ϕ and the horizontal orbital velocity $u(t)$ computed along 160 m, following the methodology described above. The velocity amplitude, U_w , was computed from H_s, T and the water depth, h, values, according to the linear wave theory, $U_w = \pi H_{rms}/(T\sinh(kh))$. The initial beach profile is plotted in the lower panel. For decreasing depths, the values of the orbital velocity near the bottom, U_w, generally decrease in consonance with H_s. However, in some regions the values of U_w arise. For example, the values of U_w arise between $24 < x < 40.5$ m where a plateau is observed for the wave height but the water depth values are decreasing.

The spatial variation of r and ϕ provide a good insight on how the wave nonlinearities change as the waves propagate onshore. Panels d), f), g) and h) also complement the analysis, showing the results of the horizontal orbital motions of $u(t)$ obtained with Eq. (1) at three selected cross-shore positions. At the deepest position shown ($x = 160$ m), r is practically zero corresponding to a sinusoidal motion. Further onshore, undoubtedly, the results show that nonlinearities increase (the value of r grows almost up to 0.7). This is followed by a change in the values of ϕ from $-\pi/2$ (*i.e.*, preponderance of short, high crests) to almost zero close to the shore line. This highlights the shape of the orbital motion at the most onshore positions, where the wave is pitching forward (sawtooth shape) and the acceleration skewness attains maximum values.

The three positions marked with symbols in Figure 3 correspond to the locations where the significant values of the positive (u_{max}) and negative (u_{min}) near-bed velocities were measured during the experiments ($x = 24.5$, 54.5 and 119.5 m). In such cases, it is possible to characterize the wave nonlinearities in terms of a velocity skewness coefficient, R ($= u_{max} /(u_{max} - u_{min})$).

Figure 4 compares the measured and predicted values of u_{max}, u_{min} and R along the cross-shore distance x. The predicted values agree reasonably well with the experimental data since the magnitude and the spatial distribution of the three parameters is well described. This indicates that the combination of the selected parameterizations of Abreu *et al.* (2010) and Ruessink *et al.* (2012) capture efficiently the observed wave transformations, providing a good characterization of the flow which is required for the morphodynamic computations.
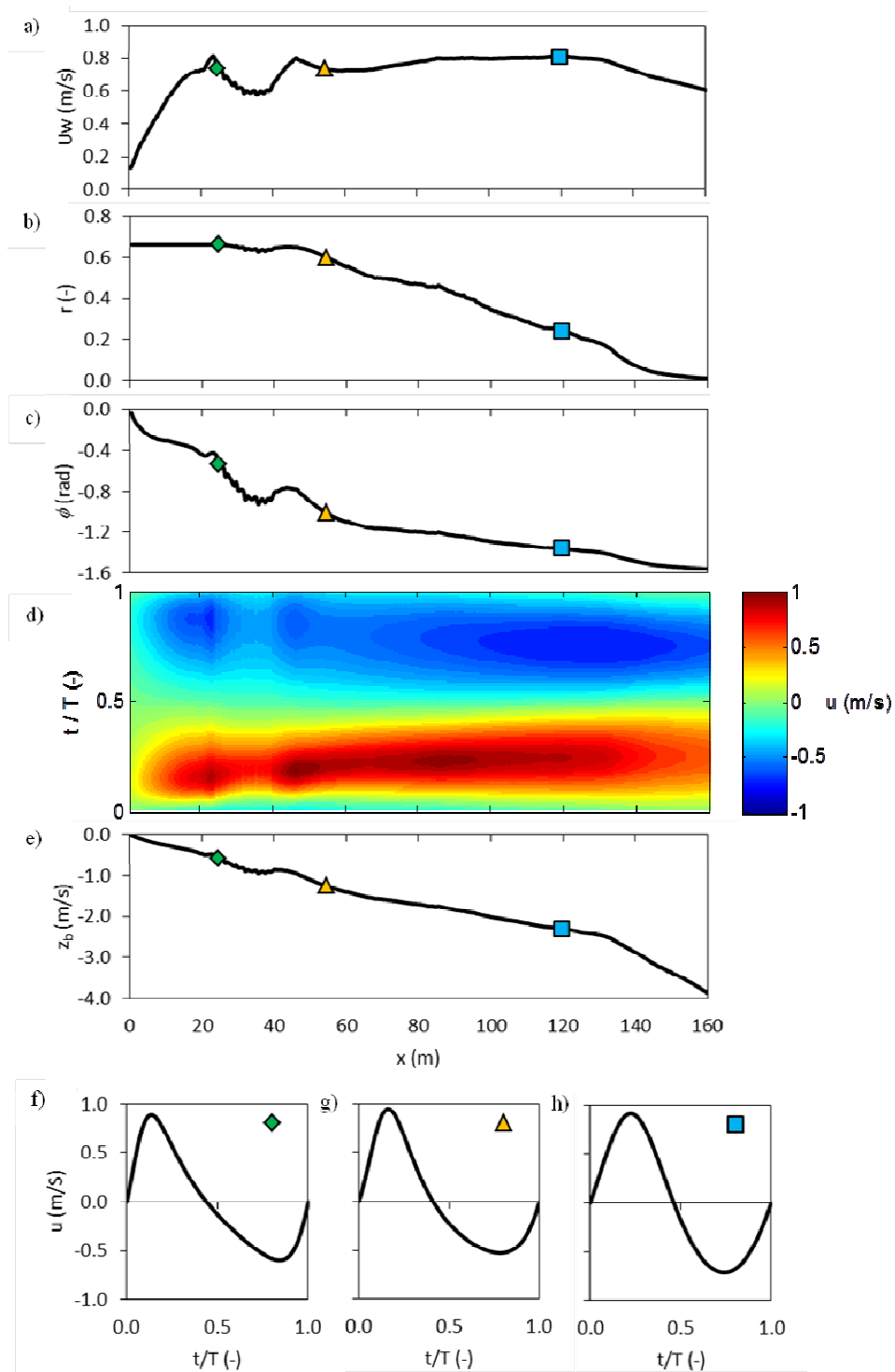
Figure 3. (a) Linear wave, near-bed, orbital velocity U_w, (b) non-linearity parameter r, (c) waveform parameter, ϕ, (d) horizontal velocity $u(t)$ and (e) bed elevation z_b *versus* cross-shore distance x. Panels (f), (g) and (h) show the temporal variation of $u(t)$ for three cross-shore positions indicated with symbols (diamond – x =24.5 m; triangle – x= 54.5 m; rectangle – x = 119.5 m).
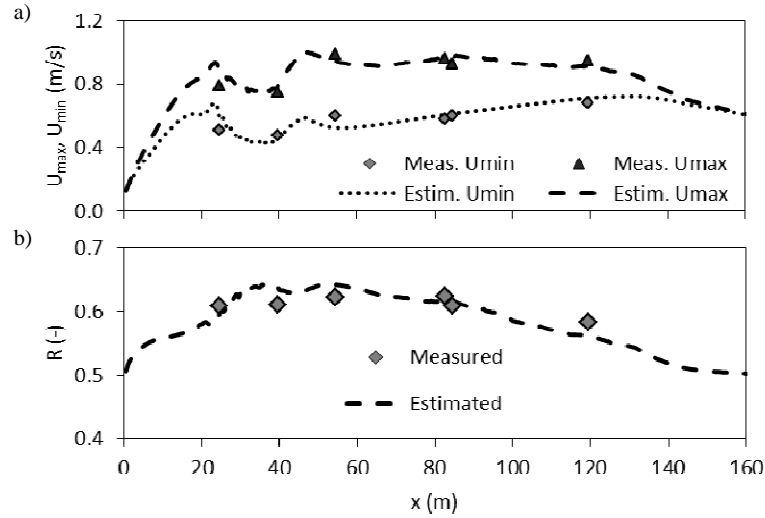
Figure 4. (a) Significant values of the horizontal flow u_{max} and u_{min} and (b) velocity skewness coefficient, R.

3.2. *Sediment transport models*

The wave-current interaction and the asymmetries of the wave shape and the induced near-bed flow are inextricably linked to the near-bed sediment dynamics (*e.g.*, Watanabe and Sato, 2004; Silva *et al.*, 2011; Dong *et al.*, 2013). The recognition of its importance to the nearshore sediment transport has also motivated the development of practical sand transport models including these processes (*e.g.*, Drake and Calantoni, 2001; Hoefel and Elgar, 2003; Nielsen, 2006; Silva *et al.*, 2006; van Rijn, 2007). Here, some sediment transport formulas were selected in order to analyze its performance to predict the beach profile evolution.

In the following, the total instantaneous velocity is obtained by adding the measured (/interpolated) mean velocities, U_b, to those computed by means of Eq. (1).

3.2.1. *Bailard (1981) – B81; Hoefel and Elgar (2003) – HE03*
Bailard (1981) extended Bagnold's (1966) energetics-type sediment transport model for steady flows to include the effects of the oscillatory motion. The model was derived to include the effects of nonlinearities in the surf zone through the use of measured velocity moments as input.

Afterwards, Drake and Calantoni (2001) suggested a modification to the classical formulation of Bailard (1981), through the inclusion of an additional term, qba, in the bedload qb component, representing acceleration effects. The model solely considers bedload transport on a horizontal bed and excludes the effect of mean currents. A dimensional descriptor of the acceleration skewness, askipe, was introduced:

$$a_{spike} = \langle a^3 \rangle / \langle a^2 \rangle \,, \tag{4}$$

where the angle brackets denote a time averaging and a is the fluid flow acceleration. The transport is enhanced due to acceleration effects if a_{spike} exceeds a critical value a_{cr}.

After Drake and Calantoni (2001), Hoefel and Elgar (2003) have extended the classical energetics model to account for random waves and take into account the sign of a_{cr}. Through the comparison of model results with field observations of a sandbar migration (Duck94 field data) they have determined the optimal values for their parameterization and a critical threshold $a_{cr} = 0.2$ m/s^2. Here, the suspended load, q_{ss}, was also computed according to Bailard (1981) in order to give the total transport q_s $(= q_b + q_{ss})$.

3.2.2. *Silva et al. (2006) – S06*
Based on the work of Dibajnia and Watanabe (1992), Silva *et al.* (2006) developed a semi-unsteady, practical model, to predict the total sediment transport rates in wave or combined wave-current flows. The predicted non-dimensional transport rates, Φ, are computed from:

$$\Phi = \frac{q_s}{\sqrt{(s-1)gd_{50}{}^3}} = \alpha \ |\Gamma| \ ^\gamma \frac{\Gamma}{|\Gamma|} \tag{5}$$

with

$$\Gamma = \frac{u_c T_c (\Omega_c^3 + \Omega_t'^3) - u_t T_t (\Omega_t^3 + \Omega_c'^3)}{2(u_c T_c + u_t T_t)} . \tag{6}$$

In these equations ρ and ρ_s are the water and sediment density, respectively, $s = \rho_s / \rho$, g is the gravitational acceleration, T_c and T_t are the time duration of the positive and negative half cycle of the near bed velocity, respectively, with equivalent velocities u_c and u_t (the subscript c stands for crest and t for trough). The quantities Ω_i and Ω_i' ($i = c, t$) represent the amount of sediment that is entrained, transported and settled in the i half cycle, and the amount of sediment still in suspension from the i half cycle that will be transported in the next half cycle, respectively. The values of Ω_i are computed from the bed shear stress. The non-steady processes are taken into account through the exchange of sediment fluxes between the two half cycles (Ω_i' quantities). The parameters α and γ are two empirical constants. Their values were determined by fitting the numerical solutions to a large data set, $\alpha = 3.2$ and $\gamma = 0.55$. Further details of the model are presented in Silva *et al.* (2006).

3.2.2. *Nielsen (2006) – N06; Abreu et al. – A13*
To estimate sediment transport rates, q_s, Nielsen (2006) proposes a quasi-steady bedload formula, which is a modified version of the Meyer-Peter Müller (1948) bedload-type formula:

$$q_s = 12\sqrt{(s-1)gd^3}\left(\theta(t) - \theta_{cr}\right)\sqrt{\theta(t)}\, u_* / |u_*|, \ \ \theta > \theta_{cr} . \tag{7}$$

The Shields parameter θ is defined by $\theta(t) = \tau(t) / \left(\rho(\rho_s/\rho - 1)gd_{50}\right)$ and τ is the instantaneous bottom shear stress ($\tau(t) = \rho u_*(t)|u_*(t)|$) computed as a function of the shear velocity, u_* (Nielsen, 1992, 2002):

$$u_*(t) = \sqrt{\frac{f_w}{2}}\left(\cos(\varphi)\, u(t) + \frac{\sin(\varphi)}{\omega}\frac{du(t)}{dt}\right). \tag{8}$$

The angle φ is a calibrating parameter that, in the case of a single harmonic, roughly represents the phase lead of the bed shear stress over the free-stream velocity. The parameter establishes the balance between drag forces and pressure gradients associated with the cosine and sine of $\varphi \in [0°, 90°]$, respectively. An optimal value of $\varphi = 51°$ was proposed, which optimizes Nielsen's net transport predictions for the data of Watanabe and Sato (2004). To compute the wave friction factor, f_w, Nielsen's (1992) formulation is recommended.

Recently, Abreu *et al.* (2013) extended the work of Nielsen (1992, 2002), proposing a new formulation to predict the bed shear stress under skewed/asymmetric oscillatory flows. The shear velocity, u_*, incorporates the nonlinearity of the oscillatory flow through the inclusion of r and ϕ:

$$u_*(t) = \sqrt{\frac{f_w}{2}}\left(\cos(\varphi)\, u(t) + \frac{\sin(\varphi)}{\omega}\left[\frac{du(t)}{dt} - S(t, \phi, r)\right]\right), \tag{9}$$

with

$$S(t, \phi, r) = \omega \cdot f \cdot U_w \frac{r\left[-(-1+f)\cos\phi - 2r\cos(\omega t) + (1+f)\cos(2\omega t + \phi)\right]}{2(1+f)\left[-1 + r\cos(\omega t + \phi)\right]^2} . \tag{10}$$

Eq. (9) can be also expressed as

$$u_*(t) = \sqrt{\frac{f_w}{2}} \left(\cos(\varphi) \ u(t) - \sin(\varphi) H \left(u(t) \right) \right),$$ (11)

where $H \left(u(t) \right)$ is the Hilbert transform of $u(t)$. The advantage to rewrite Eq. (9) into Eq. (11) allows the method to be applied to any $u(t)$ for which a Hilbert transform can be defined.

Whereas Nielsen (2006) recommends the use of a phase $\varphi = 51°$ with a constant bed roughness of $k_s = 2.5d_{50}$ for sediment transport rate estimates, Abreu *et al.* (2013) show that the new bed shear stress predictor improves the measured experimental net transport rates using $\varphi = 51°$ and $k_s = 15d_{50}$.

3.3. *Morphodynamic model*

The morphological changes of this two-dimensional analysis (2D) can be obtained through the mass conservation equation:

$$\frac{dz_b}{dt} = -\frac{1}{1-\varepsilon_0} \frac{dq_s}{dx}$$ (12)

where z_b is the bed elevation and ε_0 the sand porosity. Following Thornton *et al.* (1996), one assumes $\varepsilon_0 = 0.3$.

Eq. (12) needs to be solved numerically and numerous finite different schemes can be found in the literature for such purpose. In this work, the two-step Lax-Wendroff FTCS (forward time, central space) scheme proposed by Richtmyer (1962) was adopted. This is a second order central difference scheme that requires the calculation of sediment transport rate at intermediate time levels. The Richtmyer scheme can be expressed as:

$$z_{b,i}^{k+1/2} = \frac{z_{b,i+1}^{k} + z_{b,i}^{k}}{2} - \frac{\Delta t}{2\Delta x} \frac{1}{(1-\varepsilon_0)} \left[\hat{q}_{s,i+1}^{k} - \hat{q}_{s,i}^{k} \right]$$ (13)

$$z_{b,i}^{k+1} = z_{b,i}^{k} - \frac{\Delta t}{(1-\varepsilon_0)\Delta x} \left[\hat{q}_{s,i}^{k+1/2} - \hat{q}_{s,i-1}^{k+1/2} \right]$$ (14)

where Δx is the grid spacing, Δt the time step, $z_{b,i}^{k+1}$ the updated bed elevation at time $k+1$ found from the sediment transport rate and the bed elevation at time k. The values of $\hat{q}_s$ are approximations for the sediment transport rates q_s obtained using a simple linear smoothing operator of 4th order constructed for discretized functions (Shapiro, 1975):

$$\hat{q}_{s,i} = \frac{1}{256} \left(-q_{s,i-4} + 8q_{s,i-3} - 28q_{s,i-2} + 56q_{s,i-1} + 186q_{s,i} + 56q_{s,i+1} - 28q_{s,i+2} + 8q_{s,i+3} - q_{s,i+4} \right),$$ (15)

In addition to the Shapiro smoothing and as suggested by De Vriend *et al.* (1993), a downward-sloping avalanching term was also included to compute the sediment transport rate q_s

$$\hat{q}_{s,i} = \hat{q}_{s,i} - \varepsilon_s \left| \hat{q}_{s,i} \right| \frac{dh}{dx},$$ (16)

where $\varepsilon_s = 2$ was adopted.

At the computational nodes located most seaward ($i=1$) and shoreward ($i=$end), the boundary conditions

are $h_1^{k+1} = h_1^{k+1/2}$ and $h_{end}^{k+1/2} = h_{end}^k$.

4. Results and discussion

The results concerning the numerical simulations of the morphodynamic model, using the selected sediment transport formulas, are illustrated in Figure 5. The solutions plot the morphological changes computed after 18h of simulation. The results show that the best performance is achieved using the classic formulation B81. Definitely, this formulation predicts reasonably well the seaward migration of the sand bar and the general tends of the beach profile changes. On the contrary, the results obtained with HE03, which extend the classical energetics model B81, predict an onshore migration of the bar. In this case, it seems that the introduction of the accelerations effects magnified the onshore transport. The results obtained with S06 lead to an offshore migration of the bar, but one observes a sharp growth of the bar. Moreover, the numerical solution predicts some fluctuations that are not observed in the experiments. The solutions referred to as A13 and N06 are similar, reflecting a growth of the sand bar, but no migration is observed. This results, probably, from the balance between the non-linear effects of the orbital motion and the undertow currents in sediment transport. Again, as for HE03, it is possible that the acceleration terms in these two formulations inhibit the ability to predict the offshore movement. To verify this suspicion one eliminated the acceleration effects by introducing the angle $\varphi = 0$. In such case, only drag forces are considered and the differences between N06 and A13 only lie on the bed roughness considered for the wave friction factor, *i.e.*, $k_s = 2.5d_{50}$ or $k_s = 15d_{50}$, respectively. Figure 6 reveals that the use of $\varphi = 0$ with $k_s = 2.5d_{50}$ (N06) clearly improves the predictions, even leading to better results than B81. The use of $k_s = 15d_{50}$ (A13) exaggerates the offshore migration of the bar with the sand being eroded further onshore.
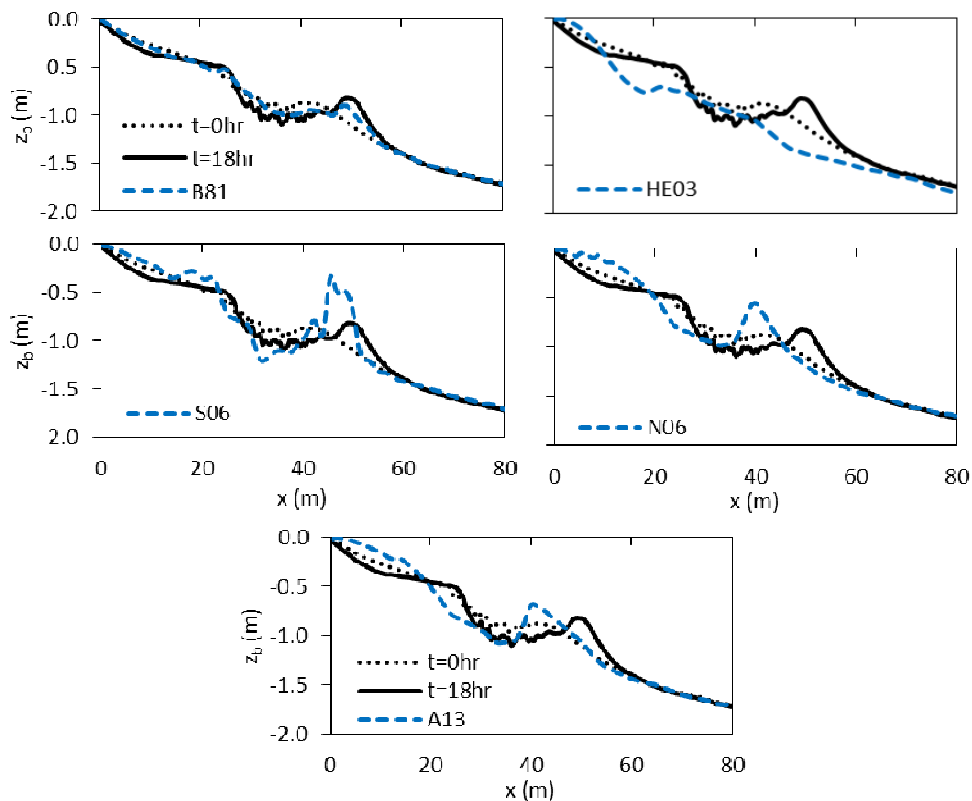

Figure 5. Experimental results (dotted and solid lines) and computed (dashed lines) profiles of 18h simulation, using the formulations of B81, HE03, S06, N06 and A13.
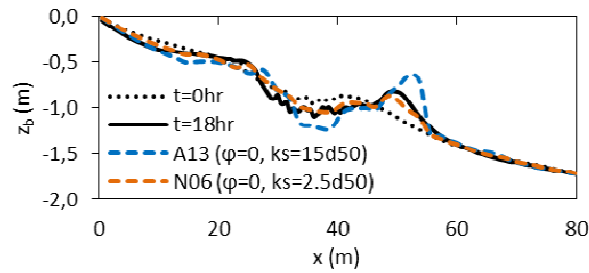
Figure 6. Experimental results (dotted and solid lines) and computed (dashed lines) profiles of 18h simulation, using the formulations of N06 and A13. The computed profiles consider the bed shear stress predictor with $\varphi = 0°$ and $k_s = 2.5d_{50}$ or $k_s = 15d_{50}$, respectively.

The results above suggest that, under these erosive conditions (offshore sand bar migration), the fluid acceleration effects in sediment transport do not seem to be as important as the orbital velocity skewness. However, such assumption may mislead to inappropriate conclusions. Indeed, the measured depth-averaged undertow was kept constant during the numerical runs and equal to the initial values. It is expected that its values changed along the experiments with the morphological changes. Also, the measured values correspond only to 9 locations in the cross-shore direction and the remaining values were obtained by linear interpolation. From the mass conservation Eq. (12) it is possible to estimate the observed net transport rates and to infer an undertow current matching that transport.

The Figure 7a shows the estimates of q_s resulting from the bed level integration between $t = 0$ and 18 hrs. Figure 7b shows the values of the undertow required to obtain the values of q_s using N06 and A13 formulations, using $\varphi = 51°$ and $k_s = 2.5d_{50}$ or $k_s = 15d_{50}$, respectively. The parameters r and ϕ used in these computations consider the initial bathymetry and were obtained as before. The U_b estimates using N06 formulation gives nearly twice the double of the estimates using A13. Noteworthy, for A13, the magnitudes of the estimated values of U_b are within the range and the uncertainty of the measured values. It is also pointed that the estimates of U_b present two peaks, which is consistent with the previous work of van Rijn *et al.* (2007) which computed the undertow for test 1B using the process-based CROSMOR profile model. Obviously, when these values are inserted for the morphodynamic simulations, both estimates of U_b lead to good predictions of the morphological changes (Figure 7c).
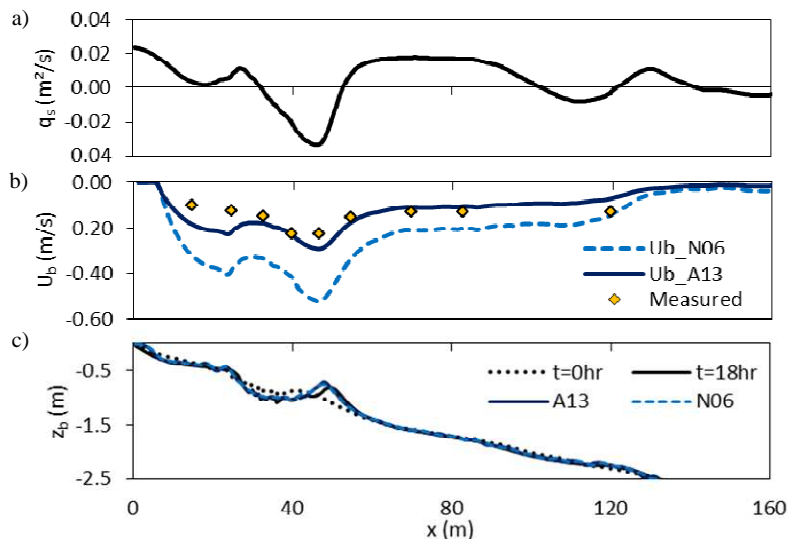

Figure 7. (a) Measured sand transport, q_s, from bed level soundings at $t=0$ and $t=18$ hr; (b) Measured (diamonds) and computed values of the undertow that lead to the values of q_s using the formulations of N06 (dashed line) and A13 (solid line).

5. Conclusions

The ability of five practical sand transport models is examined to predict beach profile evolutions. For that purpose, the numerical results of a morphodynamic model are compared against the observed beach profile evolutions during the European project "Large Installations Plan" (LIP). In this study, the LIP 1B case is investigated, corresponding to an erosive case where a breaker bar in the surf zone migrates offshore. The results enable to evidence the relative strength of mechanisms associated with the wave and current induced sand transports, as well as of the capacities and weaknesses of the selected (empirical) practical transport models.

The characterization of the orbital velocity is achieved combining the parameterizations of Abreu et al. (2010) and Ruessink et al. (2012) and the estimates are validated against the measured cross-shore velocity data. Following this methodology, a good characterization of the flow is obtained since it is seen that the orbital velocity skewness is well described. This indicates that the observed wave transformations from velocity-skewed, to acceleration-skewed in the inner surf are efficiently captured, which is an important requirement for morphodynamic computations.

Concerning the morphological changes, the classical energetics model of Bailard (1981) give the best overall results. The seaward migration of the sand bar and the general trends of the beach profile changes are well reproduced using this model. It is also seen that if the acceleration effects are neglected in Nielsen's sediment transport model good predictions are also achieved. This could point that under these erosive conditions, the effects of fluid acceleration do not seem to play an important role in sediment transport. However, these computations were performed with the undertow measured at 9 locations of the cross-shore position and the remaining values were obtained by linear interpolation. This assumption may not be appropriate and may induce to misleading conclusions. As an example, from the mass conservation equation, one computed the net transport rates and inferred the undertow current that matches the transport rates using Nielsen (2006) and Abreu et al. (2013) formulations. It is seen that in the last case the magnitudes of the estimated values of the undertow are within the range and the uncertainty of the measured values. A good estimator of the undertow seems to be crucial in such morphodynamic computations.

In the future, further validation will be pursued against field or laboratory data, exploring the results of the morphodynamic model and improving the hydrodynamic description, mainly of the mean flow.

Acknowledgements

References

Abreu, T., Silva, P.A., Sancho, F. and Temperville, A., 2010. Analytical approximate wave form for asymmetric waves, *Coastal Engineering*, 57: 656-667.

Abreu, T., Silva, P.A. and Sancho, F., 2011. Asymmetrical waves in barred beaches. *Revista de Gestão Costeira Integrada / Journal of Integrated Coastal Zone Management*, 11(3), 297-306 (in Portuguese).

Abreu, T., Michallet, H., Silva, P.A., Sancho, F., van der A, D.A. and Ruessink, B.G., 2013. Bed shear stress under skewed and asymmetric oscillatory flows. *Coastal Engineering*, 73: 1-10.

Arcilla, A. Roelvink, J., O'Conner, B., Reniers, A. and Jiménez, J., 1994. The delta flume '93 experiment. *Coastal Dynamics'94*, ASCE: 488-502.

Bagnold, R.A., 1966. An approach to the sediment transport problem from general physics. *US Geological Survey Washington*, USA.

Bailard, J.A., 1981. An energetics total load sediment transport model for a plane sloping beach. *Journal of Geophysical Research*, 86(C11): 10938–10954.

Baldock, T.E., Manoonvoravong, P., Kim Son Pham, 2010. Sediment transport and beach morphodynamics induced by free long waves, bound long waves and wave groups. *Coastal Engineering*. 57: 898–916.

De Vriend, H.J., J. Zyserman, J. Nicholson, J.A. Roelvink, P. Pechon, and Southgate, H.N., 1993. Medium-term 2DH

coastal area modeling. *Coastal Engineering*, 21: 193-224.

Dibajnia, M. and Watanabe, A., 1992. Sheet flow under nonlinear wavesand currents. *Proceedings of the 23rd International Conference on Coastal Engineering*. ASCE, Venice, Italy: 2015– 2028.

Dibajnia, M., Moriya, T. and Watanabe, A., 2001. A representative wave model for estimation of nearshore local transport rate. *Coastal Engineering Journal*, 43(1): 1-38.

Doering, J.C. and Bowen, A.J., 1995. Parametrization of orbital velocity asymmetries of shoaling and breaking waves using bispectral analysis. *Coastal Engineering*, 26(1-2): 15-33.

Dong, L.P., Sato, S. and Liu, J., 2013. A sheetflow sediment transport model for skewed-asymmetric waves combined with strong opposite currents. *Coastal Engineering*, 71: 87–101.

Drake, T.G. and Calantoni, J., 2001. Discrete particle model for sheet flow sediment transport in the nearshore. *Journal of Geophysical Research*, 106, C9: 19859-19868.

Elfrink, B., Hanes, D.M. and Ruessink, B.G., 2006. Parameterization and simulation of near bed orbital velocities under irregular waves in shallow water. *Coastal Engineering*, 53: 915-927.

Elgar, S.L. and Guza, R.T., 1985. Observations of bispectra of shoaling surface gravity waves, *Journal of Fluid Mechanics*,167: 425-448.

Hoefel, F. and Elgar, S., 2003. Wave-induced sediment transport and sandbar migration. *Science*, 299: 1885-1887.

Holman, R.A. and Bowen, A.J., 1982. Bars, bumps and holes: Models for generation of complex beach topography. *Journal of Geohysical Research*, 87: 457-468.

Malarkey, J. and Davies, A.G., 2012. Free-stream velocity descriptions under waves with skewness and asymmetry. *Coastal Engineering*, 68: 78-95.

Meyer-Peter, E. and Müller, R., 1948. Formulas for bed-load transport. *Report from the 2nd Meeting of the International Association for Hydraulic Structures Research*, Stockholm, Sweden. IAHR: 39–64.

Nielsen, P. 1992. *Coastal Bottom Boundary Layers and Sediment Transport*, Advanced Series on Ocean Engineering, 4, World Scientific, 324 pp.

Nielsen, P. 2002. Shear stress and sediment transport calculations for swash zone modelling, *Coastal Engineering*, 45(1): 53-60.

Nielsen, P. 2006. Sheet flow sediment transport under waves with acceleration skewness and boundary layer streaming. *Coastal Engineering*, 53(9): 749-758.

Prel, P., Michallet, H. and Barthélemy, E. 2011. Flume experiments on wave non-linear interactions effects on beach morphodynamics. *Journal of Coastal Research*, SI 64: 2053 - 2057.

Richtmyer, R.D., 1962. *A survey of difference methods for nonsteady fluid dynamics*, Natl. Cent. Atmos. Res. Tech., Note 63-2.

Rocha, M., Silva, P., Michallet, H., Abreu, T., Moura, D. and Fortes, C.J. (2013). Parameterizations of wave nonlinearity from local wave parameters: a comparison with field data. *Journal of Coastal Research*, SI 65: 374-379

Roelvink, J.A. and Reniers, A.J.H.M., 1995. *LIP 11D Delta Flume experiments, a profile dataset for profile model validation*. Report H2130. The Netherlands: Delft Hydraulics.

Ruessink, B.G., Ramaekers, G. and L.C. van Rijn. 2012. On the parameterization of the free-stream non-linear wave orbital motion in nearshore morphodynamic models. *Coastal Engineering*, 65: 56–63.

Sancho, F., Abreu, T., D'Alessandro, F., Tomasicchio, G.R. and Silva, P.A., 2011. Surf hydrodynamics in front of collapsing coastal dunes. *Journal of Coastal Research*, SI 64: 144-148.

Shapiro, R., 1975. Linear filtering. *Mathematics of computation*, 29 (132): 1094-1097.

Silva, P.A., Temperville, A. and Seabra Santos. F., 2006. Sand transport under combined current and wave conditions: A semi-unsteady, practical model. *Coastal Engineering*, 53(11): 897-913.

Silva, P.A., Abreu, T., van der A, D.A., Sancho, F., Ruessink, B.G., van der Werf, J.J. and Ribberink, J.S., 2011. Sediment transport in non-linear skewed oscillatory flows: Transkew experiments. *Journal of Hydraulic Research*, 49, sup1: 72-80.

Swart, D.H., 1974. *Offshore sediment transport and equilibrium beach profiles*. Publ. No. 131, Delft. Hydraulics Lab, Delft, The Netherlands, 302 pp.

Thornton, E.B., Humiston, R.T. and Birkemeier, W., 1996. Bar/trough generation on a natural beach. *Journal of Geophysical Research*, 101(C5): 12097-12110.

van Rijn, L.C., 2007. Unified View of Sediment Transport by Currents and Waves. I: Initiation of Motion, Bed Roughness, and Bed-Load Transport. *Journal of Hydraulic Engineering*, 133(6): 649-667.

van Rijn, L.C., Ruessink, B.G., Grasmeijer, B.T., van der Werf, J.J. and Ribberink, J.S., 2007. Wave-related transport and nearshore morphology. *Proc. Coastal Sediments `07*, ASCE, New Orleans, Louisiana, Vol I: 1-14.

Watanabe, A. and Sato, S. 2004. A sheet-flow transport rate formula for asymmetric, forward-leaning waves and currents. *Proceedings of the 29th International Conference on Coastal Engineering*, ASCE, Lisbon, Portugal: 1703-1714.